BIOELECTRICITY
Volume 1, Number 4, 2019

DOI: 10.1089/bioe.2019.0030

Using Nanosecond Shocks for Cardiac Defibrillation

Johanna U. Neuber, MS,[1,2] Frency Varghese, PhD,[3] Andrei G. Pakhomov, PhD,[1] and Christian W. Zemlin, PhD[1,2]

Abstract

The purpose of this review article is to summarize our current understanding of the efficacy and safety of cardiac defibrillation with nanosecond shocks. Experiments in isolated hearts, using optical mapping of the electrical activity, have demonstrated that nanosecond shocks can defibrillate with lower energies than conventional millisecond shocks. Single defibrillation strength nanosecond shocks do not cause obvious damage, but repeated stimulation leads to deterioration of the hearts. In isolated myocytes, nanosecond pulses can also stimulate at lower energies than at longer pulses and cause less electroporation (propidium uptake). The mechanism is likely electroporation of the plasma membrane. Repeated stimulation leads to distorted calcium gradients.

Keywords: defibrillation, nanosecond, cardiac, arrhythmia

Introduction

Short intense electric shocks have long been the method of choice to terminate ventricular fibrillation[1–5]. The current clinical standard is to deliver biphasic shocks of ~ 10 ms duration,[6–9] either through electrode panels placed on the thorax[10] or in patients known to be at risk for fibrillation, through an implanted defibrillation device with electrodes close to and inside the heart.[11] Adverse effects of conventional defibrillation may include increased morbidity and mortality, anxiety, pain, and cell damage.[12–14]

Since the time when defibrillation was introduced, important aspects of the mechanisms of defibrillation have been elucidated,[15–19] and particular effort has been put into finding shock wave forms that would allow effective defibrillation at lower energies.[20,21] This research led to the replacement of the original monophasic truncated exponential waveforms by the biphasic waveforms that are used today.[22–24] More recently, trains of low-amplitude shocks have shown potential to achieve defibrillation at lower energies.[25,26]

A relatively new approach is to use shocks that are much shorter than conventional pulses, that is, nanosecond duration shocks. Such shocks have previously been used to ablate tissue, including cardiac tissue.[27,28] They are also effective to defibrillate the heart, at higher field strength but lower energy than conventional shocks.[29] Whether nanosecond defibrillation has a place in clinical practice will depend on whether shock parameters can be identified that reliably defibrillate and cause less adverse effects than conventional defibrillation.

Defibrillation is a spatiotemporal process,[30] and the efficacy of nanosecond defibrillation can only be fully assessed in cardiac tissue. Isolated cardiomyocytes are still an important model to study defibrillation because stimulation can be used as a proxy for defibrillation. Stimulation is a viable proxy on theoretical grounds, because the success of defibrillation depends on whether a shock activates enough of the cardiac tissue[15,16,31] (but our data hereunder suggest that it has limitations). Stimulation of individual myocytes with nanosecond pulses is possible,[32,33] and the mechanism of stimulation likely involves electroporation of the plasma membrane.[33,34] The possible adverse effects of electric shocks can be assessed both in isolated myocytes and in cardiac tissue. The main mechanism of damage is electroporation,[14,34–36] and since the pores formed by nanosecond shocks tend to be smaller than those formed by millisecond shocks,[37–41] the electroporative damage may also be reduced. In this study, we summarize experimental methods and results on nanosecond defibrillation, both from whole hearts and isolated myocyte experiments.

Ex Vivo Defibrillation Setup

Heart preparation

Nanosecond defibrillation can be studied with the same approach as conventional defibrillation, in a Langendorff setup[42] (Fig. 1A). Hearts are excised, the aorta is quickly cannulated, and the heart flushed with cold cardioplegic solution to avoid ischemic damage. The heart is then placed in an experimental chamber filled with 37°C Tyrode solution,

[1]Frank Reidy Research Center for Bioelectrics, Old Dominion University, Norfolk, Virginia.
[2]Department of Electrical and Computer Engineering, Old Dominion University, Norfolk, Virginia.
[3]Department of Medicine, University of Massachusetts Medical School, Worcester, Massachusetts.

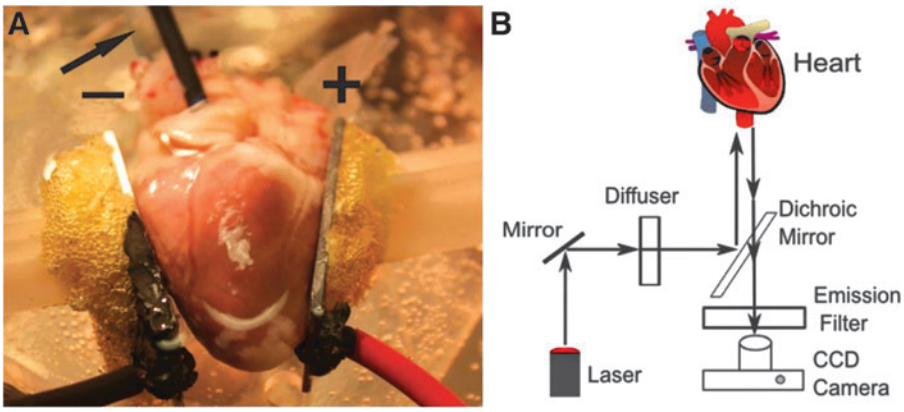

FIG. 1. Experimental setup for *ex vivo* defibrillation studies and optical mapping setup. **(A)** Heart preparation. An excised rabbit heart is perfused and superfused with Tyrode's solution. Aluminum plate electrodes, labeled ''+'' (anode) and ''–'' (cathode), are placed in contact with the heart on the left and right ventricles. The arrow is pointing to the transparent cannula that perfuses the heart; the black tube next to the cannula is inserted through the left atrial wall into the left ventricle to provide an outlet from the left ventricle (since the aorta is cannulated). The yellow foamy substance between the electrodes and the (white) manipulators is water-insoluble glue used for mounting the electrodes. **(B)** Optical mapping setup. Laser light is diffused and directed toward the heart to excite the fluorescent dye. The fluorescent light then passes the dichroic mirror and an emission filter and is recorded by a CCD camera. CCD, charge-coupled device.

whereas the aorta is also retrogradely perfused with oxygenated 37°C Tyrode solution at controlled pressure (50–80 mmHg).

Optical mapping

To record the electrical signals of the heart, a voltage-sensitive dye (such as a near-infrared dye DI-4-ANBDQBS) is injected as a bolus.[43] The heart is uniformly illuminated with diffused laser light to excite the fluorescence (Fig. 1B). The emitted fluorescence is separated from the excitation light with a dichroic mirror and filters and recorded with a high-speed camera. In this way, the electrical activity within the field of view of the camera is monitored. The excitation and emission wavelength of the dye determine how much the superficial and deeper layers contribute to the optical signal.[44] During a spontaneous or stimulated activation of the heart, the electrical activity consists of a single activation wave that traverses the heart; during ventricular fibrillation, a multitude of small transient waves move across the heart in a complex pattern. By monitoring the fluorescence of a single pixel, which corresponds to a surface element of the heart, the transmembrane voltage as a function of time in this location can be obtained. Optical mapping with voltage-sensitive fluorescent dyes is the gold standard for measuring the spatially resolved electrical activity of the heart.[45]

Induction of fibrillation

Several pacing patterns have been suggested to induce fibrillation, including burst pacing or incremental pacing (increasing the stimulation rate).[46–49] Another popular and effective method is to gently touch the surface of the heart with both poles of a 9 V battery.[50,51] These methods are typically effective in inducing fibrillation, but depending on the species and the size of the heart, fibrillation may not be sustained. To make fibrillation more sustained, some studies add pinacidil (5–10 μM), an agonist of the ATP-dependent K^+-channel that shortens the action potential.[52,53] Defibrillation efficacy should be tested on hearts that are experiencing episodes of sustained fibrillation, which can be defined as fibrillation that has continued for 30 s after induction.

Shock application

To mimic the field distribution during a defibrillation shock that is delivered through electrode panels on the thorax, two planar electrodes are placed on opposite sides of the heart (Fig. 1).[29] Nanosecond or millisecond shocks are delivered through these electrodes. Typical impedances are 10–15 Ω for isolated rabbit hearts (2 × 2 cm electrodes, separated by 3 cm, immersed in Tyrode solution). Impedances of pulser and load should be matched by adding resistors in parallel or series with the load as needed.[29]

Cardiomyocyte Isolation and Stimulation

The isolation of cardiomyocytes requires species-specific buffers and protocols. For isolation of mouse, rabbit, and pig cardiomyocytes, see Ref.[54] In brief, hearts were harvested and immediately arrested, and cardiomyocytes were isolated by enzymatic digestion during Langendorff perfusion (using type II collagenase or Liberase™). Cells were then seeded onto glass coverslips. A pair of rod electrodes (e.g., tungsten) was used to apply electrical pulses.

To measure calcium transients, a calcium-sensitive fluorescent dye was added to the medium, and fluorescence measured under a microscope.[33,38,54,55] The electromechanical uncoupler blebbistatin was added to the medium to prevent movement artifacts and propidium iodide (PI) was added to measure membrane permeability.

Efficacy of Nanosecond Defibrillation

Shocks of 300 ns duration can reliably terminate fibrillation in isolated rabbit hearts.[29] Nanosecond shocks were applied in 12 hearts to determine the defibrillation threshold. The dose–response curve for nanosecond shocks, shown in Figure 2, follows a sigmoidal curve that is also typical for

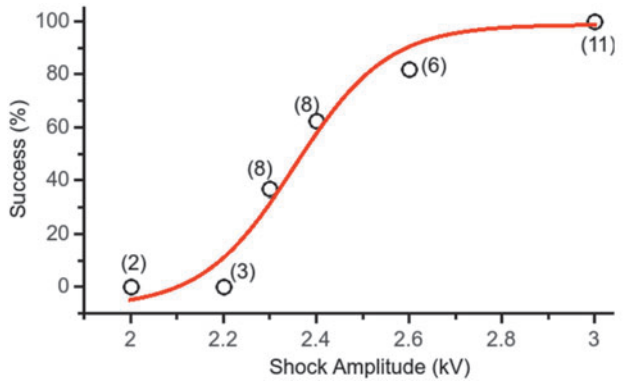

FIG. 2. Defibrillation success rate as a function of shock amplitude for single 300 ns shocks. The number of observations contributing to each data point is shown in parentheses. The red line is a sigmoidal curve fitted to the data. Reproduced from Varghese et al.[29] courtesy of Springer.

conventional defibrillation. ED_{50} of defibrillation, defined as the shock amplitude for which the fitted success probability is 50%, was determined to be 2.35 kV (ED_{50} is also referred to as the ''defibrillation threshold''[56]). For shocks of 3 kV amplitude, every defibrillation attempt was successful (11/11).

To compare the required energy of nanosecond and millisecond defibrillation, ED_{50} was determined for both modalities in the same hearts.[29] The energy W delivered by a millisecond shock was computed by recording the current $I(t)$ with a Pearson probe and computing $W = I(t)U(t)dt$, whereas the energy delivered by nanosecond shocks was computed assuming that the capacitor used in the delivery discharged completely, $W = \frac{CU_c^2}{2}$, where C is the capacitance of the charged capacitor and U_C is the charging voltage. The average energy required for nanosecond defibrillation was 64 ± 4 mJ, compared with 530 ± 35 mJ for millisecond defibrillation. This indicates that nanosecond defibrillation is possible with profoundly reduced energy.

Damage from Nanosecond Defibrillation

To determine whether successful nanosecond defibrillation is accompanied by electroporation damage, hearts were harvested and immediately perfused with Tyrode solution with added PI (20 μg/mL).[29] Then a single 3 kV 300 ns shock was applied (this shock strength corresponds to 100% defibrillation success; Fig. 2). Hearts were sectioned and PI fluorescence was evaluated. No PI uptake was evident in any section of any heart (four sections each in six hearts), indicating that there was no electroporative damage. In addition, after the end of the experiments, sections were stained with triphenyl tetrazolium chloride.[27] All hearts ($n = 6$) exhibited uniform staining of the tissue, indicating that all tissue remained metabolically active.

To detect possible more subtle damage, optical mapping traces were also examined for signs of electrophysiological changes.[29] When a single defibrillation strength shock was applied to a heart in sinus rhythm, there was no significant change in the duration of the subsequent action potentials. The diastolic interval (DI) directly after the shock increased by >50%, but this change was transient: the second DI returned to normal. It should be noted that conventional defibrillation also causes a transient elongation of the DI.[57] The shock effect was uniform over the heart, that is, the tissue in the immediate vicinity of the electrodes did not respond differently from the tissue distal from them.

Optical mapping traces of defibrillation strength shocks applied to fibrillating hearts[29] were also examined. Although this setting is especially interesting because it replicates the situation in which shocks would really be applied, it has the disadvantage that action potential durations (APDs) and DIs cannot be compared with their preshock values, because there is no regular preshock activity. Still, it is possible to determine, for both of APDs and DIs, whether they are stationary immediately after the shock or take time to stabilize after the shock. Consistent with the stimulation results, APDs were stationary immediately after the shock, whereas the DI was prolonged by >50% immediately after the shock but stationary starting from the second beat.

Optical mapping traces were also checked for baseline shift, which would indicate electroporation, but it was absent in all recordings.[29] An electrode with a window onto which an indium tin oxide (ITO)-coated cover slip was mounted was also used to record the activity right underneath the shock electrode. Even in this setting, there was no baseline shift.

Another index of the amount of damage that nanosecond shocks cause is how many such shocks the heart can receive and still exhibit normal electric activity. During experiments to determine the stimulation threshold of nanosecond shocks of 200 to 1000 ns duration, hearts were repeatedly exposed to nanosecond shocks close to the stimulation threshold. Hearts received an average of 215 ± 30 ns stimulations before the heart deteriorated to the point that stimulation attempts were discontinued. These experiments were conducted in our laboratory and have not been previously published.

Nanosecond Stimulation of Whole Hearts

Since defibrillation is damaging for the heart, a large number of hearts are required to obtain dose–response curves such as that shown in Figure 2, even for a single shock duration. To determine which other shock durations are promising candidates, the stimulation threshold can be used as a proxy for the ED_{50} of defibrillation. Many more of the weaker stimulation pulses can be applied in a single heart, and since defibrillation essentially succeeds whenever a sufficient part of the tissue is activated by the shock, it is reasonable to expect that ED_{50} for defibrillation depends on the shock duration in a similar way as the stimulation threshold.

In experiments to determine the stimulation threshold from the nanosecond range to milliseconds, hearts were paced with millisecond pulses through plate electrodes, and a single pulse was replaced with a pulse of the duration of interest, after which millisecond pacing was resumed. As expected, the stimulation threshold (electric field) increased with decreasing pulse duration (Fig. 3). When the stimulation energy was calculated by integrating the product of the current and voltage waveforms, there was a minimum at 100 μs, making this pulse duration promising for further evaluation.

At the same time, there are several remarkable features shown in Figure 3 that illustrate the limitations of our current understanding of nanosecond stimulation. The dependence of the electric field on the pulse duration is linear on a log–log scale from 0.1 to 100 μs (Fig. 3), with a slope of

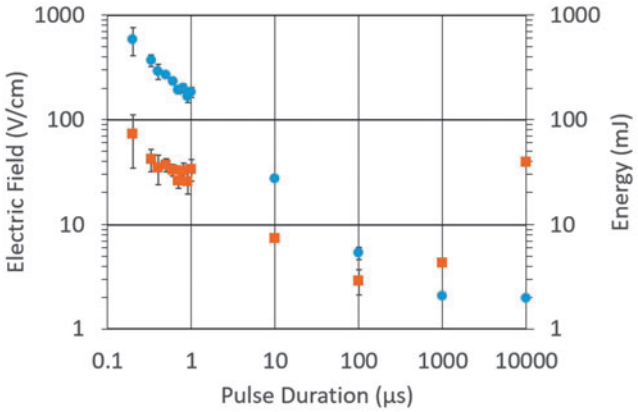

FIG. 3. The strength–duration curve of the electric field (blue circles) and corresponding energies (orange squares) for stimulation with monophasic shocks with durations from 200 ns to 10 ms ($n=6$).

approximately −0.75, indicating $E \sim d^{-0.75}$. As we discuss hereunder in the section on the mechanism of nanosecond defibrillation, a power of −1 or lower would be expected here. Also, the energy required for 300 ns and 10 ms stimulation is almost identical, whereas the energy required for *defibrillation* with 300 ns pulses is 8 times lower, as already discussed. This indicates that the use of the stimulation threshold as a proxy for ED_{50} of defibrillation has serious limitations.

Nanosecond Stimulation of Isolated Cardiomyocytes

Nanosecond stimulation of cardiomyocytes resulted in calcium transients with no difference in shape (rise time and decay time constant) compared with millisecond stimulation.[54] This suggests that nanosecond pulses induce excitation in a manner similar to conventional stimuli, by charging the cell membrane.

The strength–duration curve for the stimulation threshold was measured from 200 ns to 2 ms in rabbit, pig, and mouse cardiomyocytes.[54] As expected, the electric field threshold increased as the pulse duration decreased. The shortest duration tested, 200 ns, required the least energy for stimulation. In addition, when cells were challenged with a single pulse at five times the stimulation threshold, the least PI uptake was observed at 200 ns (Fig. 4).

A separate study found that nanosecond stimulation caused both calcium entry into cardiac myocytes, including routes other than voltage-gated calcium channels, and slow sustained depolarization (SSD).[33] Tetrodotoxin-sensitive action potentials were mediated by SSD, whose amplitude depended on the calcium entry. Plasma membrane electroporation was the most likely primary mechanism of SSD with additional contribution from L-type calcium and sodium–calcium exchanger currents.

When repeat stimulation (5 pulses at 2 Hz) was attempted with nanosecond pulses, only the first stimulation reliably yielded a normal calcium transient.[54] Subsequent pulses frequently either failed to elicit a response or caused distorted calcium transients.[54] Such distortions can also occur after 0.2 ms pulses, but they are much less common.

Reconciling Whole Heart and Isolated Myocyte Results

The data from whole hearts seem to contradict those from isolated myocytes in three aspects: the amount of damage inflicted by nanosecond shocks, the likely mechanism by

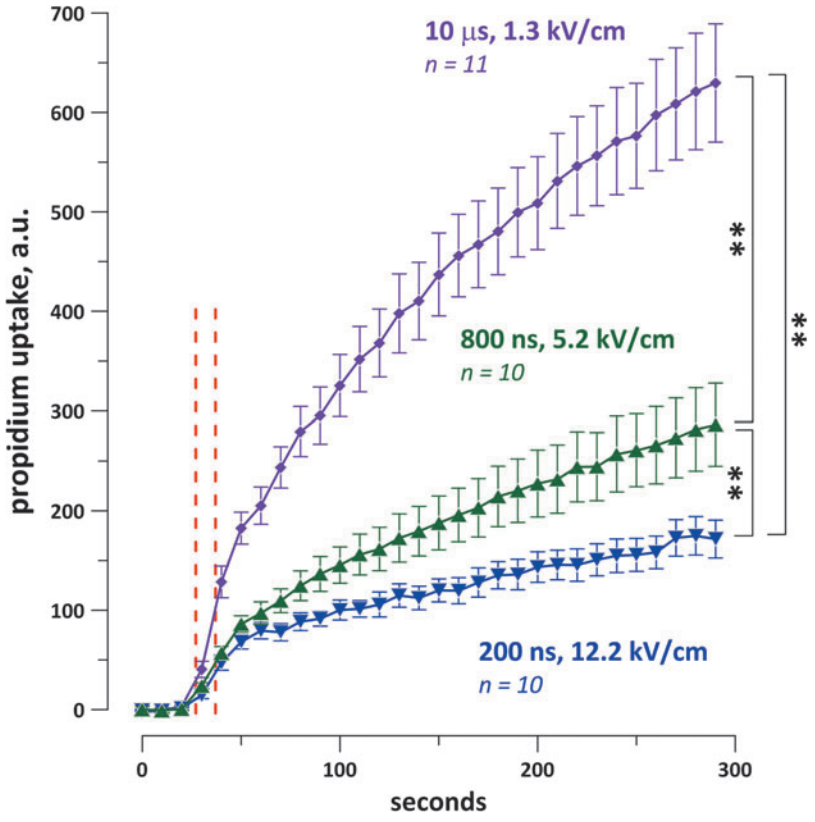

FIG. 4. Propidium iodide uptake of rabbit cardiomyocytes after a single shock at five times the threshold for calcium transient activation for each cell. The dashed red lines indicate the interval during which the shocks were applied. The shock duration, average electric field values, and the number of experiments are shown next the traces. $^{**}p<0.01$ with a two-tailed Student's t-test. Reproduced from Semenov et al.[54] courtesy of Springer Nature.

which they stimulate, and whether nanosecond pulses require more or less energy than microsecond pulses for stimulation.

As already reported, damage in whole hearts only became substantial after >200 pulses of stimulation strength, and single defibrillation strength shocks caused no detectable tissue death or permanent electrophysiological changes. In contrast, isolated myocytes often showed clear signs of electroporation even after a small number of stimulations. A possible explanation is that stimulation of a whole heart only requires that the pulse stimulates (and damages) a small subset of all the cardiomyocytes in the heart, which can, in turn, stimulate the remaining myocytes. Therefore, the damage of a single whole heart stimulation would be undetectable, but hundreds of stimulations would lead to detectable damage. In this context, it is also interesting to note that we have observed the recovery of individual myocytes that have been damaged by nanosecond stimulation, typically over tens of minutes. This recovery mechanism should increase the resilience of whole hearts to nanosecond stimulation.

Regarding the mechanism of stimulation, results in individual cardiomyocytes indicate that electroporation is likely responsible, whereas no signs of such electroporation were observed in whole heart stimulation. Again, we think that the most likely explanation is that electroporation does occur in whole heart stimulation, but that the fraction of the cells affected is too small to allow detection with optical mapping, which averages the signals of many cells.

The energy required for stimulation in single cell experiments was lower for shorter pulses in all the species considered (mouse, rabbit, and pig). In whole hearts, the minimum energy was required for 100 μs pulses. The cause for this discrepancy is currently unknown.

The pulse shapes typically used in whole heart[29] and single cell experiments[58] are approximately trapezoidal, with rise and fall time in the range of 5–20% of the pulse duration; we do not expect that differences in pulse shape are responsible for substantial changes in stimulation results as those already discussed.

Mechanism of Nanosecond Stimulation

Nanosecond shocks are capable of stimulating and defibrillating cardiac tissue, but the mechanism by which excitation occurs is still unknown. In general, a transmembrane potential is elicited by either dielectric charging or by conductive charging through the movement of ions.

Dielectric charging occurs when dipoles (mostly water in this case) align in the electric field, which results in a net movement of charge and a change in transmembrane voltage. In the case of cardiomyocytes, however, the induced field is not large enough to reach the stimulation threshold. For example, for 300 ns pulses, Figure 3 shows that the stimulation threshold is 585 V/cm. For a membrane thickness of 5 nm and a gain factor of 20 (the ratio of the permittivities of water and membrane), the induced change in transmembrane voltage is only 5.85 mV.[29] This is insufficient for activation, particularly since the change in membrane potential due to dielectric charging only lasts as long as the duration of the pulse.

Membrane charging by the movement of ions remains as the likely mechanism, but the dependence of the stimulation threshold on the pulse duration shown in Figure 3 is hard to explain within this context. If a fixed total movement of membrane charge is required to stimulate a cell, the product of pulse duration d and charging current I should be constant, or $I \sim d^{-1}$. Since the current is the product of the constant carrier density n and carrier velocity v, $I = n \cdot v$, we should further have $v \sim d^{-1}$. The movement of a carrier in an electric field (drift) is described by the equation $v = \mu E$, where μ is the mobility (assumed to be constant) and E the electric field, so we would expect $E \sim d^{-1}$. Deviations from the exponent -1 in this relationship for small d would be expected to go to more negative values (such as -1.1), because as ions move faster and faster, they start to lose energy in more types of interactions and should, therefore, require a stronger field to maintain their speed.[59] In Figure 3, however, we observe and exponent of -0.75, indicating that a weaker field than expected is sufficient to compensate for the shorter pulse and suggesting that cooperative processes may be involved.

Similarly, for stimulation of tissue with millisecond pulses, it was reported that the charging time ''constant'' drops substantially as the pulse amplitude increases.[60,61] This also implies that shorter pulses with the associated higher field strengths are more effective than expected in charging the membrane. If the charging time constant should drop down to values in the 10–100 μs range for nanosecond stimulation, membrane charging may account for the stimulation and defibrillation thresholds we observe here. However, further experiments are needed to confirm this explanation.

Conclusion and Outlook

Defibrillation with nanosecond shocks is possible at energies almost an order of magnitude lower than conventional defibrillation. Single defibrillation strength shocks did not cause observable electroporation and had only benign and transient effects on the electrophysiological behavior, but repeated stimulation with hundreds of pulses led to deterioration of the heart. In isolated cardiomyocytes, stimulation with nanosecond pulses required less energy and led to less PI uptake, but repeated stimulation quickly led to distorted calcium transients. A way to avoid damage due to nanosecond stimulation may lie in the new approach of applying high-frequency bursts of nanosecond pulses (MHz compression) instead of single pulses, which dramatically lowers the stimulation threshold and separates it from membrane damage threshold.[55] The effect of varying shock duration on the ED_{50} of defibrillation is incompletely understood, and further studies are needed to establish optimal parameters for nanosecond defibrillation. The path to clinical applications will require studying nanosecond defibrillation in isolated large animal hearts (pigs and dogs are the most commonly used species) and ultimately *in vivo* nanosecond defibrillation in large animals.

Authors' Contributions

J.N. wrote the first draft of the article. F.V and A.G.P. gave detailed comments and participated in multiple discussions to improve the draft. C.Z. led the discussion and wrote several revisions as well as the final article. All authors have reviewed and approved the article before submission.

Author Disclosure Statement

A patent application for defibrillation with nanosecond shocks is pending, with A.G.P. and C.W.Z. as inventors.

Funding Information

The research described in this review was supported by R01HL128381 from NHLBI (to A.G.P.) and 17PRE33660500 from AHA (to J.N.).

References

1. Gutbrod SR, Efimov IR. A shocking past: A walk through generations of defibrillation development. IEEE Trans Biomed Eng 2014;61:1466–1473.
2. Dosdall DJ, Fast VG, Ideker RE. Mechanisms of defibrillation. Annu Rev Biomed Eng 2010;12:233–258.
3. Truong HT, Low LS, Kern KB. Current approaches to cardiopulmonary resuscitation. Curr Probl Cardiol 2015;40: 275–313.
4. Bhanji F, Donoghue AJ, Wolff MS, et al. Part 14: Education: 2015 American Heart Association Guidelines Update for Cardiopulmonary Resuscitation and Emergency Cardiovascular Care. Circulation 2015;132:S561–S573.
5. Viereck S, Palsgaard Moller T, Kjaer Ersboll A, et al. Effect of bystander CPR initiation prior to the emergency call on ROSC and 30 day survival-An evaluation of 548 emergency calls. Resuscitation 2017;111:55–61.
6. Martens PR, Russell JK, Wolcke B, et al. Optimal response to cardiac arrest study: Defibrillation waveform effects. Resuscitation 2001;49:233–243.
7. Behrens S, Li C, Kirchhof P, et al. Reduced arrhythmogenicity of biphasic versus monophasic T-wave shocks. Implications for defibrillation efficacy. Circulation 1996; 94:1974–1980.
8. Ristagno G, Yu T, Quan W, et al. Current is better than energy as predictor of success for biphasic defibrillatory shocks in a porcine model of ventricular fibrillation. Resuscitation 2013;84:678–683.
9. Bardy GH, Marchlinski FE, Sharma AD, et al. Multicenter comparison of truncated biphasic shocks and standard damped sine wave monophasic shocks for transthoracic ventricular defibrillation. Transthoracic Investigators. Circulation 1996;94:2507–2514.
10. Ley SJ. Cardiac surgical resuscitation: State of the science. Crit Care Nurs Clin North Am 2019;31:437–452.
11. Nichol G, Sayre MR, Guerra F, et al. Defibrillation for ventricular fibrillation: A shocking update. J Am Coll Cardiol 2017;70:1496–1509.
12. Bradfield JS, Buch E, Shivkumar K. Interventions to decrease the morbidity and mortality associated with implantable cardioverter-defibrillator shocks. Curr Opin Crit Care 2012;18:432–437.
13. Cook SC, Marie Valente A, Maul TM, et al. Shock-related anxiety and sexual function in adults with congenital heart disease and implantable cardioverter-defibrillators. Heart Rhythm 2013;10:805–810.
14. Al-Khadra A, Nikolski V, Efimov IR. The role of electroporation in defibrillation. Circ Res 2000;87:797–804.
15. Mower MM, Mirowski M, Spear JF, et al. Patterns of ventricular activity during catheter defibrillation. Circulation 1974;49:858–861.
16. Chen PS, Shibata N, Dixon EG, et al. Activation during ventricular defibrillation in open-chest dogs. Evidence of complete cessation and regeneration of ventricular fibrillation after unsuccessful shocks. J Clin Invest 1986;77: 810–823.
17. Efimov IR, Cheng Y, Yamanouchi Y, et al. Direct evidence of the role of virtual electrode-induced phase singularity in success and failure of defibrillation. J Cardiovasc Electrophysiol 2000;11:861–868.
18. Zemlin C, Mironov S, Pertsov A. Delayed success in termination of three-dimensional reentry: Role of surface polarization. J Cardiovasc Electrophysiol 2003;14:S257–S263.
19. Pertsov AM, Zemlin CW, Hyatt CJ, et al. What can we learn from the optically recorded epicardial action potential? Biophys J 2006;91:3959–3960.
20. Gurvich NL, Yuniev GS. Restoration of heart rhythm during fibrillation by a condenser discharge. Am Rev Sov Med 1947;4:252–256.
21. Lown B, Kleiger R, Wolff G. The technique of cardioversion. Am Heart J 1964;67:282–284.
22. Clark CB, Zhang Y, Davies LR, et al. Transthoracic biphasic waveform defibrillation at very high and very low energies: A comparison with monophasic waveforms in an animal model of ventricular fibrillation. Resuscitation 2002;54:183–186.
23. Kudenchuk PJ, Cobb LA, Copass MK, et al. Transthoracic incremental monophasic versus biphasic defibrillation by emergency responders (TIMBER): A randomized comparison of monophasic with biphasic waveform ascending energy defibrillation for the resuscitation of out-of-hospital cardiac arrest due to ventricular fibrillation. Circulation 2006;114:2010–2018.
24. Mittal S, Ayati S, Stein KM, et al. Comparison of a novel rectilinear biphasic waveform with a damped sine wave monophasic waveform for transthoracic ventricular defibrillation. J Am Coll Cardiol 1999;34:1595–1601.
25. Rantner LJ, Tice BM, Trayanova NA. Terminating ventricular tachyarrhythmias using far-field low-voltage stimuli: Mechanisms and delivery protocols. Heart Rhythm 2013;10:1209–1217.
26. Luther S, Fenton FH, Kornreich BG, et al. Low-energy control of electrical turbulence in the heart. Nature 2011; 475:235.
27. Xie F, Varghese F, Pakhomov AG, et al. Ablation of myocardial tissue with nanosecond pulsed electric fields. PLoS One 2015;10:e0144833.
28. Xie F, Zemlin CW. Effect of twisted fiber anisotropy in cardiac tissue on ablation with pulsed electric fields. PLoS One 2016;11:e0152262.
29. Varghese F, Neuber JU, Xie F, et al. Low-energy defibrillation with nanosecond electric shocks. Cardiovasc Res 2017;113:1789–1797.
30. Keener JP, Panfilov AV. A biophysical model for defibrillation of cardiac tissue. Biophys J 1996;71:1335–1345.
31. Boukens BJ, Gutbrod SR, Efimov IR. Imaging of ventricular fibrillation and defibrillation: The virtual electrode hypothesis. Adv Exp Med Biol 2015;859:343–365.
32. Wang S, Chen J, Chen MT, et al. Cardiac myocyte excitation by ultrashort high-field pulses. Biophys J 2009;96:1640–1648.
33. Azarov JE, Semenov I, Casciola M, et al. Excitation of murine cardiac myocytes by nanosecond pulsed electric field. J Cardiovasc Electrophysiol 2019;30:392–401.
34. Wang CH, Lee YH, Kuo HT, et al. Dielectrophoretically-assisted electroporation using light-activated virtual microelectrodes for multiple DNA transfection. Lab Chip 2014;14: 592–601.

35. Tovar O, Tung L. Electroporation and recovery of cardiac cell membrane with rectangular voltage pulses. Am J Physiol 1992;263:H1128–H1136.
36. Tung L. Electroporation of cardiac cells. Methods Mol Biol 1995;48:253–271.
37. Pakhomov AG, Pakhomova ON. Nanopores: A distinct transmembrane passageway inelectroporated cells. In: Pakhomov AG, Miklavcic D, Markov MS, eds. Advanced Electroporation Techniques in Biology in Medicine. Boca Raton: CRC Press, 2010.
38. Semenov I, Zemlin C, Pakhomova ON, et al. Diffuse, nonpolar electropermeabilization and reduced propidium uptake distinguish the effect of nanosecond electric pulses. Biochim Biophys Acta 2015;1848:2118–2125.
39. Bowman AM, Nesin OM, Pakhomova ON, et al. Analysis of plasma membrane integrity by fluorescent detection of Tl(+) uptake. J Membr Biol 2010;236:15–26.
40. Nesin OM, Pakhomova ON, Xiao S, et al. Manipulation of cell volume and membrane pore comparison following single cell permeabilization with 60- and 600-ns electric pulses. Biochim Biophys Acta 2011;1808:792–801.
41. Gowrishankar TR, Weaver JC. Electrical behavior and pore accumulation in a multicellular model for conventional and supra-electroporation. Biochem Biophys Res Commun 2006;349:643–653.
42. Zemlin CW, Bernus O, Matiukas A, et al. Extracting intramural wavefront orientation from optical upstroke shapes in whole hearts. Biophys J 2008;95:942–950.
43. Matiukas A, Mitrea BG, Qin M, et al. Near-infrared voltage-sensitive fluorescent dyes optimized for optical mapping in blood-perfused myocardium. Heart Rhythm 2007;4:1441–1451.
44. Caldwell BJ, Wellner M, Mitrea BG, et al. Probing field-induced tissue polarization using transillumination fluorescent imaging. Biophys J 2010;99:2058–2066.
45. Berenfeld O, Efimov I. Optical Mapping. Card Electrophysiol Clin 2019;11:495–510.
46. Lukl J, Marek D, Bulava A, et al. Prolonged burst as a new method for cardioverter-defibrillator testing. EP Europace 2012;15:55–59.
47. Cao JM, Qu Z, Kim YH, et al. Spatiotemporal heterogeneity in the induction of ventricular fibrillation by rapid pacing: Importance of cardiac restitution properties. Circ Res 1999;84:1318–1331.
48. Banville I, Chattipakorn N, Gray RA. Restitution dynamics during pacing and arrhythmias in isolated pig hearts. J Cardiovasc Electrophysiol 2004;15:455–463.
49. Jiang H, Zhao D, Cui B, et al. Electrical restitution determined by epicardial contact mapping and surface electrocardiogram: Its role in ventricular fibrillation inducibility in swine. J Electrocardiol 2008;41:152–159.
50. Euler DE, Whitman TA, Roberts PR, et al. Low voltage direct current delivered through unipolar transvenous leads: An alternate method for the induction of ventricular fibrillation. Pacing Clin Electrophysiol 1999;22:908–914.
51. Bishop MJ, Burton RA, Kalla M, et al. Mechanism of reentry induction by a 9-V battery in rabbit ventricles. Am J Physiol Heart Circ Physiol 2014;306:H1041–H1053.
52. Chi L, Black SC, Kuo PI, et al. Actions of pinacidil at a reduced potassium concentration: A direct cardiac effect possibly involving the ATP-dependent potassium channel. J Cardiovasc Pharmacol 1993;21:179–190.
53. Fagbemi SO, Chi L, Lucchesi BR. Antifibrillatory and profibrillatory actions of selected class I antiarrhythmic agents. J Cardiovasc Pharmacol 1993;21:709–719.
54. Semenov I, Grigoryev S, Neuber JU, et al. Excitation and injury of adult ventricular cardiomyocytes by nano- to millisecond electric shocks. Sci Rep 2018;8:8233.
55. Pakhomov AG, Xiao S, Novickij V, et al. Excitation and electroporation by MHz bursts of nanosecond stimuli. Biochem Biophys Res Commun 2019;518:759–764.
56. Davy JM, Fain ES, Dorian P, et al. The relationship between successful defibrillation and delivered energy in open-chest dogs: Reappraisal of the ''defibrillation threshold'' concept. Am Heart J 1987;113:77–84.
57. Deakin CD, Ambler JJ. Post-shock myocardial stunning: A prospective randomised double-blind comparison of monophasic and biphasic waveforms. Resuscitation 2006;68:329–333.
58. Pakhomov AG, Grigoryev S, Semenov I, et al. The second phase of bipolar, nanosecond-range electric pulses determines the electroporation efficiency. Bioelectrochemistry 2018;122:123–133.
59. Matthiessen A. On the electric conducting power of the metals. Philos Trans R Soc London 1858;148:383–387.
60. Mowrey KA, Cheng Y, Tchou PJ, et al. Kinetics of defibrillation shock-induced response: Design implications for the optimal defibrillation waveform. Europace 2002;4:27–39.
61. Mowrey KA, Efimov IR, Cheng Y. Membrane time constant during internal defibrillation strength shocks in intact heart: Effects of Na+ and Ca2+ channel blockers. J Cardiovasc Electrophysiol 2009;20:85–92.

Address correspondence to:
Christian W. Zemlin, PhD
Frank Reidy Research Center for Bioelectrics
Old Dominion University
4211 Monarch Way
Norfolk, VA 23508

E-mail: czemlin@odu.edu